Received: 21 July 2021 | Revised: 28 September 2021 | Accepted: 7 October 2021

DOI: 10.1002/ecs2.3906

ECOSPHERE
AN ESA OPEN ACCESS JOURNAL

ARTICLE

Emerging Technologies

Remote sensing to characterize inundation and vegetation dynamics of upland lagoons

James Brinkhoff[1] | Gillian Backhouse[2] | Manu E. Saunders[2] | Deborah S. Bower[2] | John T. Hunter[2]

[1]Applied Agricultural Remote Sensing Centre, University of New England, Armidale, New South Wales, Australia

[2]School of Environmental and Rural Science, University of New England, Armidale, New South Wales, Australia

Correspondence
James Brinkhoff
Email: james.brinkhoff@une.edu.au

Funding information
Australian Research Council, Grant/Award Number: DE200101424; Glen Innes Natural Resources Advisory Committee; Local Land Services Northern Tablelands; NSW Environmental Trust

Handling Editor: David Bell

Abstract

Understanding broad trends in the distribution and composition of wetlands is essential for making evidence-based management decisions. Determining temporal change in the extent of inundation in wetlands using remote sensing remains challenging and requires on-ground verification to determine accuracy and precision. Therefore, optimization and validation of remote sensing methods in threatened wetlands is a high priority for their conservation. Despite their ecological importance in the landscape, we have little knowledge of the variation in the spatial extent of inundation in upland lagoons, a threatened ecological community in New South Wales, Australia. Our project developed locally trained algorithms to predict the extent of water and emergent vegetation using imagery from the Landsat-5, -7, and -8 satellites. The best model for upland lagoons used shortwave infrared reflectance (performing better than normalized difference spectral indices), with model accuracy against validation transects greater than 95%. We applied the model to images from 1988 to 2020 across 58 lagoons to generate a dataset that demonstrates the variable water regime and vegetation change in response to local rainfall over 32 years such as in the lagoons. Our results reduce threats to a dynamic threatened ecological community by filling an important knowledge gap and demonstrate a valuable method to understand historical and current changes in the hydrology of dynamic wetland systems more broadly.

KEYWORDS

ecosystem communities, ephemeral wetlands, inundation monitoring, Landsat, remote sensing

INTRODUCTION

Anthropogenic influences have destroyed over 33% of the world's wetlands (Davidson, 2014; Hu et al., 2017) and many remain threatened by changing land uses and climate change (Erwin, 2009; Reis et al., 2017). A global loss of wetlands has contributed to a large decline in freshwater biota (Reid et al., 2019), which is often highly endemic (Dudgeon et al., 2006). In addition, the ecological services of wetlands including water storage, flood mitigation, and nutrient regeneration rely on well-functioning aquatic ecosystems (Kingsford et al., 2016). Therefore, to mitigate the further decline of wetlands and the services they provide, identifying and understanding broad trends in wetland distribution and composition is essential. Useful survey methods must be able to quantify the water regime (spatial and temporal change in water), and vegetation cover of wetlands on a landscape scale. This is particularly important within regions of the world with low and unpredictable rainfall, such as Australia, where wetting and drying cycles can be highly variable and difficult to monitor (Hunter & Lechner, 2017; Lechner et al., 2016). Wetlands in such locations may wet seasonally, intermittently, or episodically as short flush events or extend over days to years (Schael et al., 2015).

Remote sensing provides a useful tool to analyze temporal change in the landscape because it can retrospectively capture differences, making use of a rich historical archive of satellite imagery. Remote sensing models to quantify the extent of water in wetlands include a range of methods (Chasmer et al., 2020). These include synthetic aperture radar (SAR) data, which is insensitive to cloud cover and sensitive to water (Montgomery et al., 2019), but historical coverage is limited (Alonso et al., 2020). Moderate Resolution Imaging Spectroradiometer data are available from 2000; however, the resolution of 250 m is too coarse for small wetland monitoring (Mohammadi et al., 2017). For applications that do not require an extensive historical archive, Sentinel-2 multispectral data are useful, with 10- to 20-m resolution (depending on band) and high-frequency images every 5 days or better (Lefebvre et al., 2019). However, for deeper historical analysis, Landsat data are most suitable because it covers 1984 to the present and has medium resolution (30 m for Landsat-5, -7, and -8) (Kissel et al., 2020).

Spectral indices derived from Landsat data combine reflectances from multiple image bands that enable the detection of specific surface characteristics. Many studies have mapped inundation extent by quantifying optimal thresholds of spectral indices for local conditions (Inman & Lyons, 2020; Thomas et al., 2015). The modified normalized difference water index (MNDWI) often provides the best predictions of open water (Ji et al., 2009; Xu, 2006). While MNDWI detects permanent water, Gao's NDWI (otherwise known as the land surface water index [LSWI]) (Gao, 1996) is better at detecting seasonal water but may be complicated by vegetation in the ecosystem (Campos et al., 2012). Wetland characteristics including water depth, turbidity, and vegetation structure affect measured spectral properties and different spectral algorithms perform better at discriminating between water, nonwater, and emergent vegetation under different conditions (Campos et al., 2012; Lefebvre et al., 2019; Roshier & Rumbachs, 2004). Therefore, to ensure sufficient classification accuracy, spectral algorithms should be developed and validated in local conditions.

General water classifiers can be useful at the landscape scale, by utilizing large training datasets to fit multivariate decision trees (Fisher et al., 2016; Mueller et al., 2016). Decision trees have advantages over other machine learning methods such as random forest and support vector regression, in that they are somewhat interpretable. However, they need careful validation to ensure they are not overfit to the training data, which results in poor prediction when generalizing to new data (Géron, 2017).

In contrast to these works focusing on spectral indices and multivariate models, the reflectance of single bands, notably shortwave infrared (SWIR), can provide a more accurate discrimination between water and nonwater pixels based on a simple decision boundary (Lefebvre et al., 2019; Wolski et al., 2017). These reflectance models are especially advantageous in the presence of emergent vegetation, which often obscures detection of water (DeVries et al., 2017; Mueller et al., 2016). Hyperspectral measurements showed that SWIR reflectance accurately detects inundation below vegetation although error rates increase with increasing vegetation cover (Jones, 2015). Spectral signatures of typical water, soil, and vegetation have been successfully used to derive spectral index thresholds for pixels with pure water and mixed classes and to derive thresholds for several satellite sensors using the sensor spectral response (Ji et al., 2009). For example, for the Landsat Thematic Mapper sensors, when MNDWI was greater than 0.123, this indicated pure water pixels, and over −0.504 indicated pixels with 25% water and 75% vegetation. Despite the ongoing advances in remote sensing methods, predicted water extent in the presence of emergent vegetation has not been validated using nonimage-based validation methods for many wetlands.

Validating the most appropriate remote sensing techniques is of high priority in aquatic-threatened ecological communities (TECs) in Australia. One example of a TEC is the Upland Wetlands of the New England Tableland (commonly called upland lagoons), which have small catchments and are known to have seemingly unpredictable cycles of inundation (Hunter & Hunter, 2021; Saunders et al., 2021). The TEC is formally listed as Upland Wetlands of the Drainage Divide of the New England Tableland Bioregion under New South Wales (NSW) state legislation (Biodiversity Conservation Act 2016), and as Upland Wetlands of the New England Tablelands and the Monaro Plateau under the Australian Commonwealth Environment Protection and Biodiversity Conservation Act 1999. Here we focus on the New England Tablelands, where the TEC is represented by 58 naturally occurring wetlands in the New England region of NSW (Bell et al., 2008; Saunders et al., 2021). The NSW Department of Planning, Industry and Environment lists "Lack of knowledge and value of the TEC and the lack of understanding about the dynamics of the TEC" as a threat (New South Wales Government, 2020), yet we still do not have information on basic ecological function such as the water regime in these ecosystems. In addition, Little Llangothlin Lagoon in northern NSW is an example of an upland lagoon that is also Ramsar listed, so it is of international significance and Australia has committed to the appropriate management of such sites. To increase our capacity to monitor and understand upland lagoons, we aimed to (1) develop a model based on Landsat imagery to determine the distribution of water (including that covered by emergent vegetation) in upland lagoons; (2) validate our model using transect sampling methods, which were spatially harmonized with the Landsat pixels; and (3) use the validated model to generate a dataset of historical inundation patterns more than 30 years.

METHODS

Sites

This study was conducted in the New England Tableland bioregion of northern NSW, Australia. The bioregion has mean annual temperatures from 9 to 17°C and rainfall 653–1765 mm (NSW National Parks and Wildlife Service, 2003). Our study system, the upland lagoons, are at elevations between 900 and 1300 m, are shallow (most are <1.5 m deep), often have no inlet or outlet, and are filled by rainfall on localized catchments and at times through additional inflow by groundwater. The wetlands vary in depth and size, and the extent and duration of inundation are highly dynamic. Some upland lagoons retain water for extended periods up to decades; others may inundate only a few times a century and last only weeks. These wetlands are also known as deflation lakes based on their formation, which occurred thousands of years ago under different climatic conditions. Their formation is no longer occurring, thus they are relictual within the landscape (Bell et al., 2008). They are often characterized by a lunette on the downwind side and occur largely on basaltic soils on the NSW tablelands of the Great Dividing Range.

All 58 upland lagoons were included in our study, shown in Figure 1. They are located within an area of 13,500 km^2. The boundaries of the lagoons were delineated by on-ground observations via vegetation sampling over a 12-year period, observations of the physiography of the landscape within those visited lagoons, and interpretation of aerial imagery taken with a Leica ADS40 sensor. The median lagoon area is 0.1 km^2. There is a large range in area, with four larger than 0.9 km^2 and three smaller than 0.02 km^2.

Image collection pre-processing

All images were accessed and all image processing was performed in Google Earth Engine (GEE), which co-locates a vast data catalog with a comprehensive library of geospatial analysis tools (Gorelick et al., 2017). In GEE, we accessed analysis-ready Landsat-5, -7, and -8 surface reflectance products, which include cloud masking bands generated using USGS CFMASK code. The lagoons were covered by five tile locations, from Worldwide Reference System paths 89 and 90, and rows 80–82. All image tiles from 1988 to 2020 that intersected at least one of the lagoons was analyzed, a process that is automated in GEE. In total, 2907 tiles were processed.

Each image tile was cloud masked using the included CFMASK bands. For each lagoon, only images that were totally unmasked over the lagoon were retained. In 2012, 13 of the 58 lagoons had no images due to only Landsat-7 data being available and due to masked pixels from the scan line corrector issue of that sensor (Mueller et al., 2016). In all other years, all lagoons had at least three images, with an average of more than 21 images per year per lagoon.

The image reflectance bands that were used were green (G), red (R), near infrared (NIR), and shortwave infrared 1 (SWIR1) and 2 (SWIR2). Important normalized difference spectral indices (NDSIs) that were useful in previous wetland studies (e.g., Mohammadi et al., 2017; Xu, 2006) were calculated based on these bands. The NDSIs were defined as follows:

$$\mathrm{ND}(b1, b2) = \frac{b1 - b2}{b1 + b2}. \quad (1)$$

The NDSIs included the following:

1. Normalized Difference Vegetation Index, NDVI = ND (NIR,R) (Rouse, 1974).
2. Land Surface Water Index, LSWI = ND(NIR,SWIR1) (also known as NDWI; Gao, 1996).
3. Normalized Difference Water Index, NDWI = ND (G,NIR) (McFeeters, 1996).
4. Modified Normalized Difference Water Index, MNDWI = ND(G,SWIR1) (Xu, 2006).

The NDVI was used to describe vegetation cover, as it is related to biophysical properties such as leaf area index and biomass (Carlson & Ripley, 1997; Rouse, 1974). For

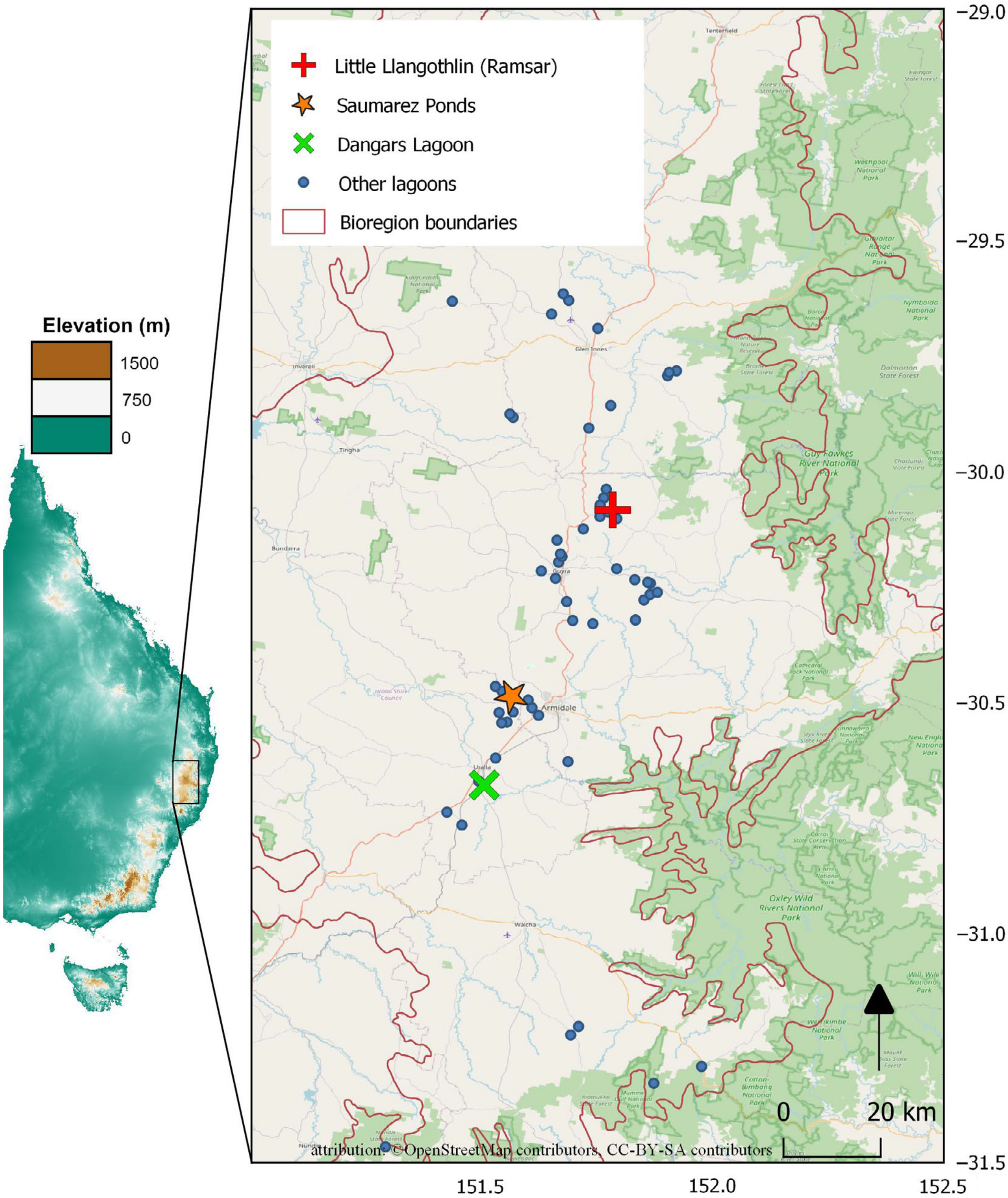

FIGURE 1 Location of the 58 dynamic lagoons in the New England Tableland bioregion of New South Wales, Australia. The selected lagoons described in detail in later sections are highlighted, including the Ramsar site

each image over each lagoon, the mean NDVI was calculated for this purpose.

Training data

Two classes were defined, *wet* and *dry*. Wet included areas with nonzero water depth, where the water may or may not be covered by vegetation, and dry included areas with zero water depth.

Training samples were generated to develop wet/dry prediction models. These were generated by specifying point locations and dates where we could be highly confident that the points were either wet or dry, using rules described in the following paragraphs. At each of these points, we extracted the reflectance and NDSI values, resulting in a table with 604 rows, for 303 dry and 301 wet points (Data S1). The table columns included class (wet/dry), and the value of all the image reflectances and NDSIs at each sample location-date. The samples included points from 13 lagoons and 29 image dates from 2009 to 2020.

In order to assign the wet/dry points, we used simple rules based on interpretation of the imagery. In addition to the RGB image, two auxiliary layers were displayed:

1. Open water. This was defined as MNDWI >0.123, which as shown by Ji et al. (2009) indicates high confidence of pure water pixels, and was similarly used by Jones (2015).
2. Vegetation. This was defined as NDVI >0.4, which Ji et al. (2009) showed could characterize the presence of at least some vegetation within a mixed pixel.

The wet and dry points were assigned to areas based on the above layers and the following rules:

1. Dry: No vegetation and no open water.
2. Wet, either:
   - Open water, or
   - Vegetation surrounded by open water. This allows the generation of samples where there must be water under vegetation (an example is shown in Figure 2) because the elevation in the area enclosed by open water is lower, due to the lagoons being saucer-shaped (Bell et al., 2008).

Example open water and vegetation layers, and training sample points, from the Little Llangothlin Lagoon for two image dates are shown in Figure 2a,b. The 2011 image was after a period with substantial rainfall, and there was a large amount of open water present in the image, with some emergent vegetation covering the water. We placed wet sample points as shown, which included areas of open water, as well as areas where the water was covered by vegetation (the presence of water is assumed due to the vegetated area being surrounded by open water as described previously). The 2019 image was in the midst of a severe drought, and there was no open water present and very little vegetation apart from trees around the edge of the lagoon, so that dry sample points could be placed with high confidence.

Inundation classification model training

We used the 604 training samples to optimize a number of decision tree classification models to predict wet and dry pixels. Though deep multivariate trees are possible (Mueller et al., 2016), or indeed ensembles of trees such as random forests (Jahncke et al., 2018), we found univariate trees with a depth of 1 were sufficient. Resulting models can be described simply by a single-decision boundary such as wet *if* SWIR1 <0.106. This simplicity provides models that are more likely to generalize to new areas and image dates, less likely to overfit training data, and are easily interpretable (Géron, 2017).

A model was generated for each of the reflectance bands and NDSIs using scikit-learn (Pedregosa et al., 2011). The wet/dry decision boundaries were optimized using the gini impurity criterion. Cross-validation was not necessary because no hyperparameters needed tuning due to the simplicity of the single-decision models. For each of the models, the number of misclassified points was calculated. This error rate gave an initial indication of the reflectance bands and NDSIs that optimally separate wet and dry pixels. Independent ground validation is described in the following section. The optimal model could then be applied to all image dates over all lagoons, giving pixel-wise predictions of inundated pixels.

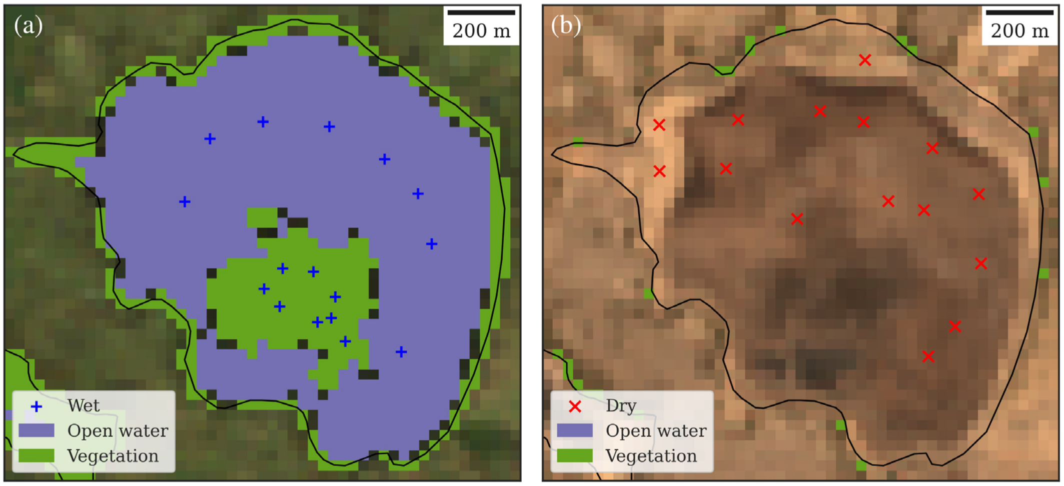

FIGURE 2 Little Llangothlin Lagoon, showing Landsat optical image in the background, and the open water and vegetation layers in the foreground. (a) Image from 8 November 2011, with entered wet training points. (b) Image from 14 November 2019, with entered dry training points

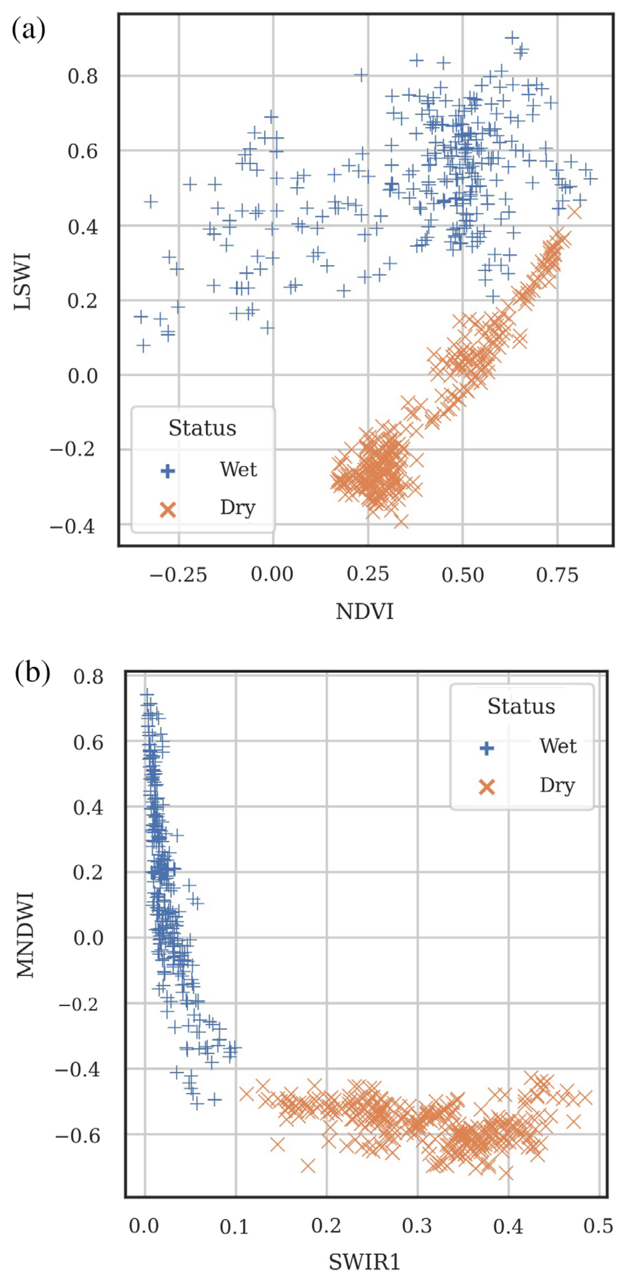

FIGURE 3 Dry and wet training sample separability using NDSIs (a, b) and the SWIR1 reflectance band (b). LSWI, land surface water index; MNDWI, modified normalized difference water index; NDVI, normalized difference vegetation index; SWIR1, shortwave infrared 1

TABLE 1 Decision boundary and error count (out of the 604 training points) for all reflectance and normalized difference spectral index (NDSI) variables

Category	Variable	Threshold	Errors
Reflectance	G	0.047	23
	R	0.049	52
	NIR	0.168	36
	SWIR1	0.106	0
	SWIR2	0.065	2
Normalized difference spectral indices	LSWI	0.230	41
	MNDWI	−0.425	5
	NDVI	0.166	236
	NDWI	−0.240	222

Abbreviations: G, green; LSWI, land surface water index; MNDWI, modified normalized difference water index; NDVI, normalized difference vegetation index; NDWI, normalized difference water index; NIR, near infrared; R, red; SWIR1, SWIR2, shortwave infrared 1 and 2.

TABLE 2 Confusion matrix between measured transects (bold) and predictions using the shortwave infrared 1 (SWIR1) band of the Landsat images (italics)

Class	Dry	Mixed	Wet	Sum	Precision (%)
Dry	104	0	0	104	100
Mixed	0	41	0	41	100
Wet	1	3	9	13	69
Sum	105	44	9	158	
Recall (%)	99	93	100		

Note: The matrix also shows the total points per class, and the precision and recall.

Transect validation data and procedure

To validate the wet/dry prediction model, we made use of a set of transect measurements that had been designed to track vegetation and water in the lagoons (Hunter & Hunter, 2021). In total, there were 158 transects (1580 plots) surveyed over 36 dates and 26 lagoons. Each transect was 50 m long, including 10 plots spaced by 5 m, with a similar layout as suggested in Chasmer et al. (2020). Each plot included 4–5 sub-plots, within which measurements of water depth and vegetation height were taken with a tape measure to the nearest centimeter in a 1 × 1-m frame. The end of each transect was geolocated using a Garmin GPSMAP 66S (sub-10-m accuracy in clear-sky conditions), and the direction of the transect was recorded using a compass. Each plot was classed as *wet* if the average water depth of the sub-plot measurements was greater than zero and *dry* if the water depth of all measurements was equal to zero.

For each transect measurement date and location, the following Landsat image with no masked pixels in the lagoon was selected. The maximum difference in date between transect measurement and image was 20 days, and the mean difference was 7.6 days. To ensure spatial and temporal independence of the training and validation datasets, none of the lagoon-date combinations were used in both datasets.

One challenge was the different spatial resolutions of the validation plots (5 m) and Landsat pixels (30 m, with typical geolocation accuracy of better than 15 m; Storey et al., 2014), making direct comparison between

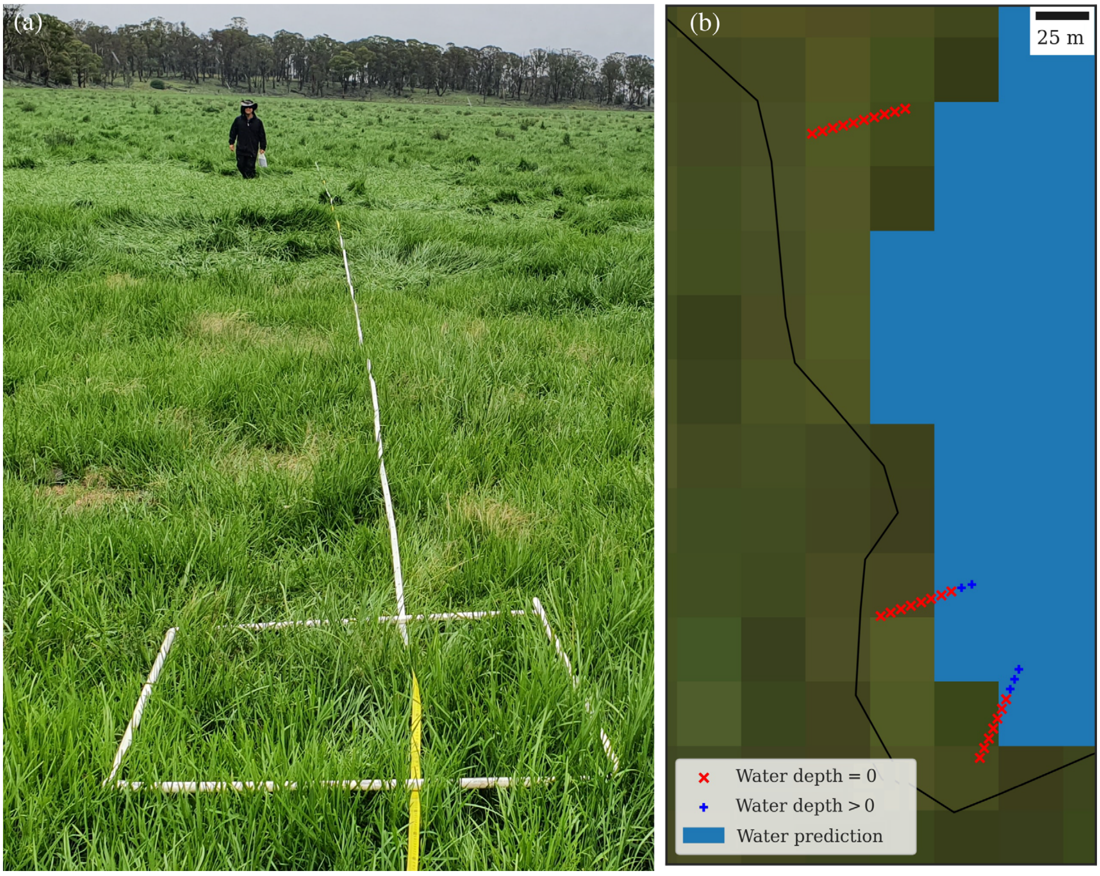

FIGURE 4 (a) Photo from a transect measurement campaign in March 2020. (b) Three validation transects (one dry and two mixed) from 3 February 2018 and image from 5 February 2018, from the western side of the Little Llangothlin Lagoon

transects and image predictions difficult. To overcome this, we created a validation dataset with one row per transect, that is, 158 rows (Data S1). The plot data and image pixel data were then aggregated for each transect. This generated three classes for the ground truth measurements and three classes for the image predictions. These three classes were as follows:

1. *Dry*. The transect measurements were classed dry if all plots were dry. The image predictions were classed dry if all pixels intersecting the transect were dry.
2. *Wet*. The transect measurements were classed wet if all plots were wet. The image predictions were classed wet if all pixels intersecting the transect were wet.
3. *Mixed*. The transect measurements were classed mixed if some plots were wet and some were dry. The image predictions were classed mixed if some pixels intersecting the transect were wet and some were dry.

The ground measurements could then be compared to the image predictions along the 158 rows to estimate prediction accuracy. We used confusion matrices and derived accuracy metrics (Foody, 2002). Metrics computed were the overall accuracy, kappa, precision, and recall.

Inundation and vegetation summary statistics

To characterize the variability of inundation and vegetation across lagoons and time, we developed summary datasets generated from the NDVI and inundation prediction pixels, at various levels of spatial and temporal aggregations:

1. Time series of vegetation and inundation percentage for each lagoon (temporal frequency defined by image dates). This was calculated using the spatial mean of pixels over each image of each lagoon.
2. Annual time series for each lagoon, by finding the yearly averages of (1).
3. Annual (min, 25th percentile, median, 75th percentile, max) over all 58 lagoons, calculated from (2).
4. Similar statistics to (3) on a seasonal (instead of annual) basis, with seasons defined as summer = December–February, autumn = March–May, winter = June–August, and spring = September–November.

Rainfall data from a weather station at Guyra were also aggregated on an annual and seasonal basis. These

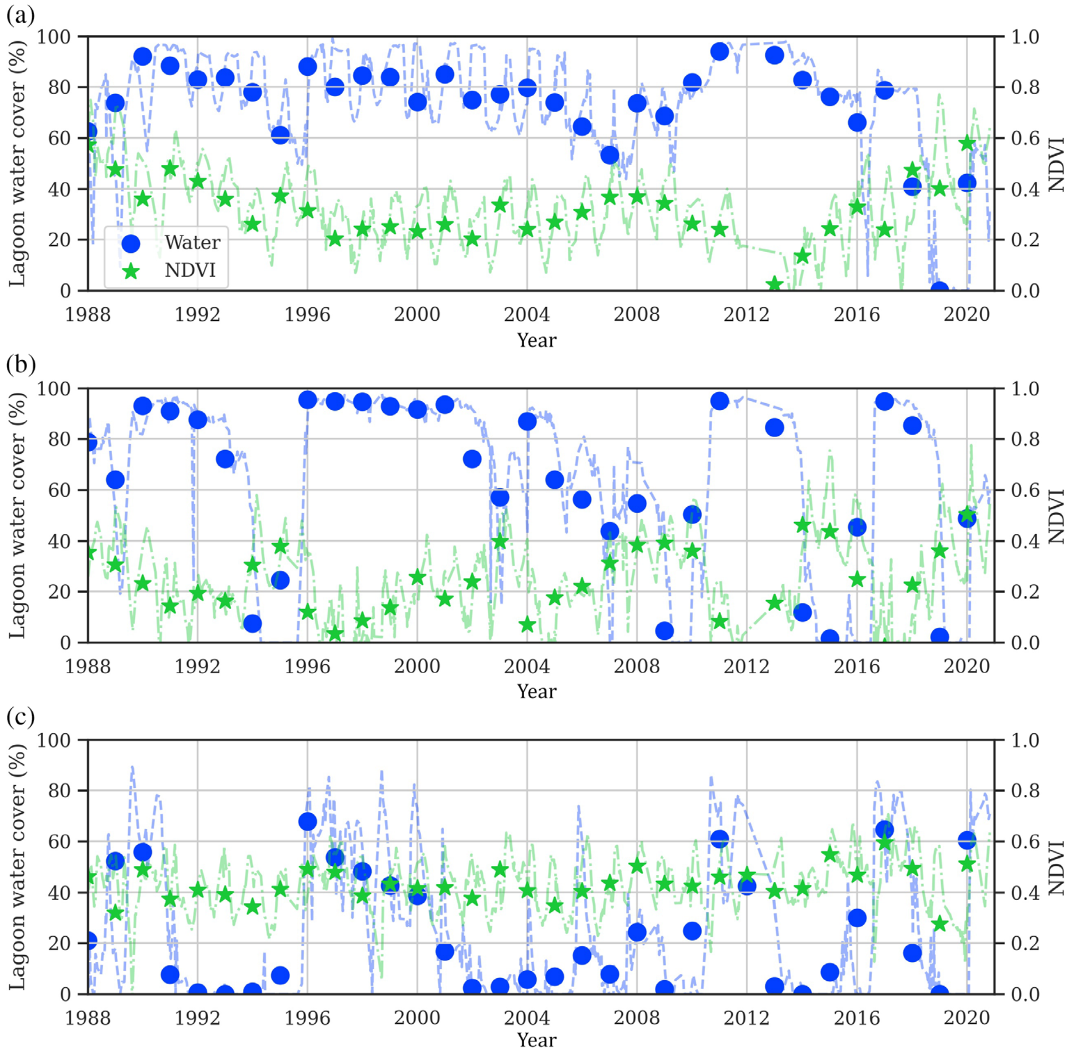

FIGURE 5 Historical water and vegetation dynamics of 3 of the 58 lagoons. Points show annual means, and lines show per-image values. (a) Little Llangothlin Lagoon. (b) Dangars Lagoon. (c) Saumerez Ponds. NDVI, normalized difference vegetation index

data provide some explanation for the annual and seasonal variability in lagoon inundation and vegetation.

RESULTS

Model selection

Due to the presence of both water and vegetation in many pixels, the dry and wet training samples of most of the NDSIs overlapped (Figure 3a). NDVI had a large range for the wet class, of which more than half of the samples overlapped with the dry class because of the presence of both open water (low NDVI) and vegetation emerging above the water surface (high NDVI). LSWI was sensitive to water and vegetation, staying above 0 for all wet samples. But dry samples also included values above 0 because of LSWI sensitivity to moisture in noninundated vegetation. Of the NDSIs, MNDWI most accurately discriminated between the wet/dry training samples. There were five wet samples that overlapped with the range in the dry class (below −0.425), which were in areas with thick vegetation (Table 1, Figure 3b).

SWIR1 was the best water predictor with 0 errors on the 604 training points and a threshold of 0.106 (Figure 3b), followed by SWIR2 with 2 errors and a threshold of 0.065. These reflectance bands are better at separating the wet/dry samples than the best NDSI (MNDWI with five errors) (Table 1).

Inundation prediction maps generated using these models, time series charts, and images of all lagoons from 1988 to present can be viewed in a GEE web app (https://jamesbrinkhoff.users.earthengine.app/view/dynamiclagoons).

Model validation

When we compared the model predictions against the transect samples measured in the field, the MNDWI

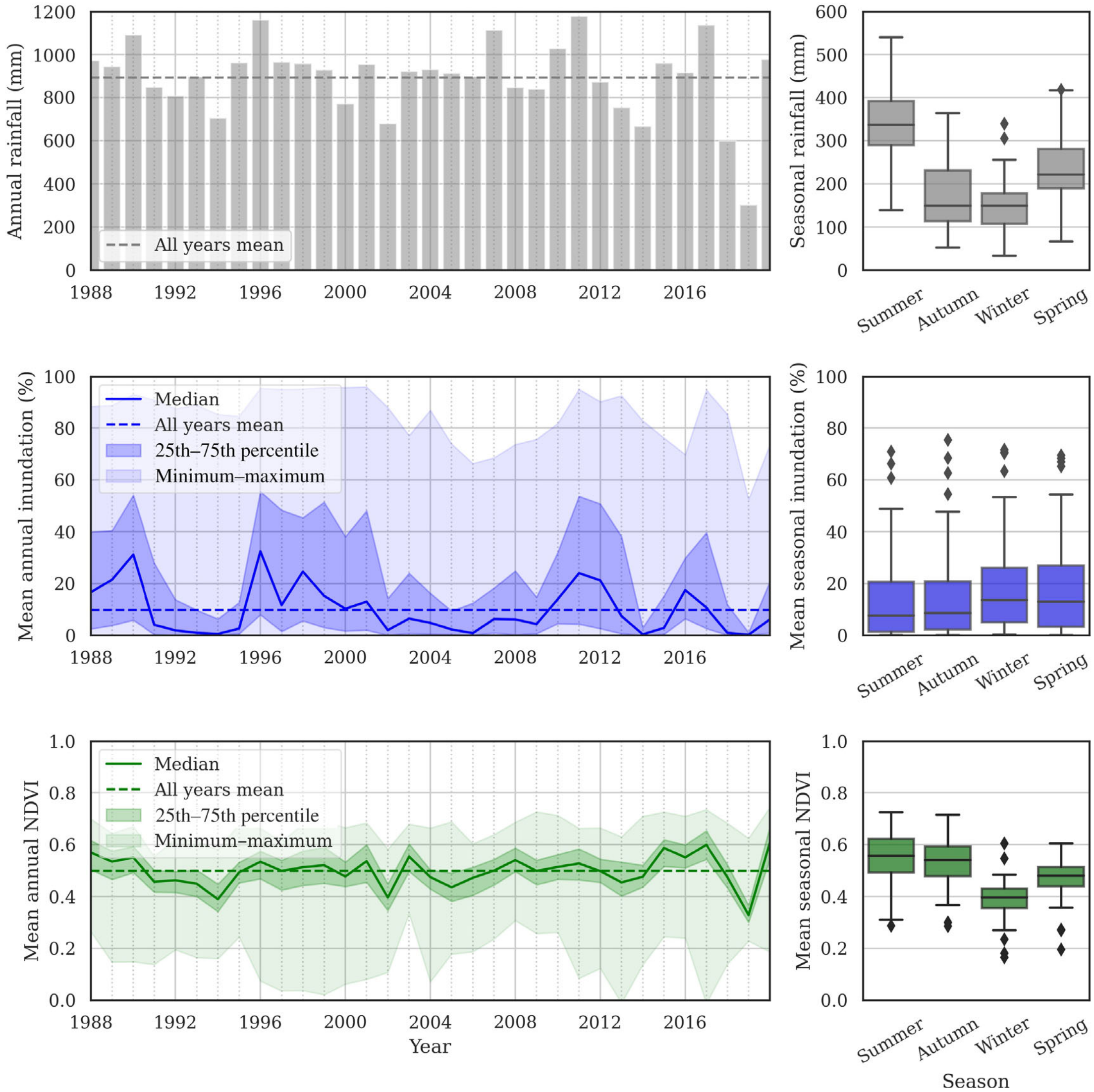

FIGURE 6 Annual and seasonal summaries of rainfall, lagoon inundation, and vegetation. The aggregations are performed per time period (year or season) over the 58 lagoons. NDVI, normalized difference vegetation index

classifier had an overall accuracy of 96.8% and kappa of 0.935. The SWIR1 classifier was more useful, with an overall accuracy of 97.5% and kappa of 0.948. All mixed and dry transect predictions were correct with 100% precision (Table 2). However, there were one dry and three mixed transects that were not predicted, with these four transects being falsely predicted as wet, therefore wet precision was 69%. In three example transects, one dry and two mixed transects were correctly identified (Figure 4b).

Inundation and vegetation trends

The case study of three selected lagoons (Appendix S1) shows the highly dynamic nature of inundation between years and among lagoons (Figure 5). The temporal pattern of the percentage of water coverage between 1988 and 2020 showed a dry period from 2002 to 2009, then a wet period in 2010–2011. More recently, there were dry periods from 2018 to 2020, with a return of more typical rainfall in late 2020.

Little Llangothlin (1.19 km^2) tended to retain water even in very dry years. Saumarez Ponds (0.25 km^2) dried out much more quickly after absence of rainfall. All three lagoons dropped to close to 0% wet area in 2019.

The relationship between water extent and vegetation varied across the lagoons. For example, in Little Llangothlin, there was a constant patch of tall sedges (*Eleocharis sphacelata*) visible in the southwest corner of the imagery (Figure 2). The NDVI of the vegetation dropped during winter, resulting in an oscillating pattern in the time series (Figure 5). The vegetation tended to obscure the detection of water in the patch during winter, resulting in erroneously low water extent predictions. In

Dangars Lagoon (Figure 5b), there was high inundation and relatively less emergent vegetation. In 2019, vegetation in all lagoons declined severely with a quick recovery after rainfall at the start of 2020.

Collectively, upland lagoons were highly variable in their water regime (Appendix S2). Some lagoons remained more than 50% inundated from 1988 to 2020, while others were usually dry (Figure 6). The effect of annual rainfall on lagoon characteristics is evident, with consecutive dry years leading to lower median inundation and vegetation. A seasonal pattern of vegetation is evident, with lower median NDVI in winter.

DISCUSSION

We tested existing remote sensing methods using data from the Landsat archive to determine the most useful model to detect water in threatened upland lagoons of the New England region in NSW, Australia. The SWIR1 model was validated using on-the-ground transects and its predictions were accurate with and without the presence of emergent vegetation. Using the SWIR1 model, we were able to assess the broad trends in long-term historical inundation patterns over 32 years for upland lagoons and detect the lagoon responses to periods of high and low rainfall. We suggest that remote sensing is applied to address knowledge gaps for other priority wetlands and that similar models will be useful for other temporary, vegetated shallow systems.

The best model for upland lagoons used a single reflectance band, SWIR1, which provided more accurate predictions than spectral-index-based models, among which the one using MNDWI was the best. The accuracy of simple reflectance band models using SWIR bands has been likewise observed in other studies (Lefebvre et al., 2019; Wolski et al., 2017). Those authors suggested the reason for this is that indices such as MNDWI are designed to detect open water, whereas the SWIR bands are better able to detect water in the presence of emergent vegetation. Given the high accuracies achieved with our single reflectance, single-decision threshold model, more complex multivariate models such as the deep decision tree adopted by Mueller et al. (2016) were not necessary. The success of our simple model may be partly due to the constrained locality and characteristics of the upland lagoons. Simple models provide the advantage of less risk of overfitting to training data and are easily interpretable.

Prediction accuracy of our model was well validated using field-sampled transects, which provided us with the confidence to interpret our model outcomes. The overall accuracy classifying the dry/mixed/wet classes was 97.5%. This was sufficient to analyze broad trends in inundation extent and emergent vegetation cover over time and has created a useful source of data to monitor the broad biophysical features of the upland lagoons.

Remote sensing models are often validated using independent and higher resolution imagery; however, using field data for validation was more powerful and allowed us to test the sensitivity and limitations of the remotely sensed data (Alonso et al., 2020; Foody, 2002). We made use of pre-existing field transect data instead of using remote sensing data for validation, as is common in other studies (Alonso et al., 2020; Thomas et al., 2011; Tulbure & Broich, 2013). The challenge we faced with making use of the field data to validate the remote sensing model was the different spatial resolutions of the validation plots (5 m) and Landsat pixels (30 m). This is a common problem faced when using field validation whether retrospective or not, because of constraints on the scale at which field data can be collected (Baccini et al., 2007). Sampling design has implications on accuracy estimation. Sampling is sometimes done in a way that all validation points are contained within a large area of the relevant ground cover away from boundaries (Jahncke et al., 2018), which leads to a potential bias towards a higher accuracy estimate (Foody, 2002). In our study, transects were placed on or near the wet/dry boundary where more classification errors were likely; however, our overall accuracy and kappa statistic were both high, and comparable to similar studies mapping inundation of wetlands within Australia using Landsat data suggesting that our method was sufficient for validation (Thomas et al., 2011; Tulbure & Broich, 2013).

The SWIR1 model was applied to all images from 1988 to 2020, and using a case study of three lagoons (Little Llangothlin, Dangars Lagoon, and Saumerez Ponds), we demonstrated the individual water regimes. The lagoons demonstrated the response of the wetlands to an extreme drought in 2019 when all lagoons dropped to almost 0% wet area. At the peak of the drought in 2019, vegetation in all lagoons declined severely with a quick recovery after rainfall at the start of 2020. The annual oscillating pattern of NDVI may be explained by above-ground biomass of emergent vegetation tending to die during winter in cold regions (Asaeda et al., 2006). A comprehensive assessment of specific lagoons also revealed that it remains challenging to detect water under emergent vegetation in difficult situations (such as the tall *E. sphacelata*), although the model was successful in most cases. Shadows due to trees overhanging smaller lagoons were misclassified as wet in some cases. Site-specific variation will always influence model accuracy, and understanding of how different environmental variables influence results in different sites is important. Fusion of multispectral data with LiDAR and SAR data is a promising direction, if such data are available at sufficient temporal and spatial resolution, and resources exist to perform the relatively complex data processing and analysis (Martinez & Letoan, 2007; Montgomery et al., 2019).

The prediction dataset demonstrated the highly dynamic nature of the New England upland lagoons over a 30-year period. The graphs demonstrated the drying effects on lagoons from droughts during 2002–2009 and 2018–2020 with intermittent wet periods such as the La Nina weather system in 2010–2011. These data are now openly accessible (https://jamesbrinkhoff.users.earthengine.app/view/dynamiclagoons), and validating the accuracy of the model now allows us to confidently monitor the water regime of upland lagoons. Development and validation of our model, in addition to the resource we have created to monitor these lagoons, provides a useful tool to help address one of the key threats to this TEC identified by the NSW Department of Planning, Industry and Environment: "Lack of knowledge and value of the TEC and the lack of understanding about the dynamics of the Threatened Ecological Community."

Historical sensor data (such as from pressure transducers or water level sensors) are not available, and the cost of implementing such systems in all 58 lagoons would be prohibitive, and indeed not possible at many sites due to them being on private land. Therefore, documenting historical changes in water regime has not otherwise been possible and our new detailed knowledge, based on freely available remote sensing data, creates the opportunity to assess the impact of changes in land use and climate change, which will be critical to inform future intervention and management. For example, there is great potential to quantify wetland dynamics using this method, and these data can then be used to build greater understanding of how land use or management factors affect wetland function. Since all lagoons have received some form of hydrological alteration and wetland function has likely been significantly altered in most lagoons (Bell et al., 2008), associating past management practices with changes over time will be a priority in research.

The temporal resolution of Landsat imagery (16 days) may be too coarse to assess extremely fine-scale watering events (e.g., illegal water extraction or small amounts of rainfall during dry periods), and the spatial resolution of Landsat imagery (30 m) is coarse relative to some of the smaller lagoons. However, our method provided the ideal technique to capture broader patterns in slower processes of wetland drying and wetting. The multidecade Landsat archive provides the means to analyze long-term wetland dynamics, and their relationship with climate variability and management factors, such as agricultural land-use change around the lagoons. This information would be valuable for conservation monitoring, especially for the single lagoon that is Ramsar listed. More recent analysis could make use of improved temporal and spatial resolution data by transferring the model to higher-resolution multispectral sensors such as Sentinel-2 (from 2015 with 20-m resolution for the crucial SWIR bands; Lefebvre et al., 2019) or SAR sensors such as Sentinel-1 (from 2014 with 10-m resolution; LaRocque et al., 2020).

We suggest that similar validation of these models should be applied to other poorly understood dynamic TECs (Saunders et al., 2021). This will enable ongoing physical monitoring of the broad patterns of water regime, allow an assessment of change over longer time frames, and create the ancillary data required for ecologists to place biodiversity research into an aquatic context.

ACKNOWLEDGMENTS

This research was funded by the NSW Government through a partnership between the Saving our Species program and the Environmental Trust and by the Australian Government through the Australian Research Council's *Discovery Early Career Researcher Award* funding scheme awarded to Deborah Bower (project DE200101424). Field survey data collection undertaken by John Hunter was funded by the Glen Innes Natural Resources Advisory Committee and the Northern Tablelands Local Land Services. The anonymous reviewers provided much useful feedback, which have resulted in significant improvements to the manuscript.

CONFLICT OF INTEREST

The authors declare no conflict of interest.

ORCID

James Brinkhoff https://orcid.org/0000-0002-0721-2458
Manu E. Saunders https://orcid.org/0000-0003-0645-8277
Deborah S. Bower https://orcid.org/0000-0003-0188-3290
John T. Hunter https://orcid.org/0000-0001-5112-0465

REFERENCES

Alonso, A., R. Munoz-Carpena, and D. Kaplan. 2020. "Coupling High-Resolution Field Monitoring and MODIS for Reconstructing Wetland Historical Hydroperiod at a High Temporal Frequency." *Remote Sensing of Environment* 247: 111807.

Asaeda, T., J. Manatunge, L. Rajapakse, and T. Fujino. 2006. "Growth Dynamics and Biomass Allocation of *Eleocharis sphacelata* at Different Water Depths: Observations, Modeling, and Applications." *Landscape and Ecological Engineering* 2(1): 31–9.

Baccini, A., M. Friedl, C. Woodcock, and Z. Zhu. 2007. "Scaling Field Data to Calibrate and Validate Moderate Spatial

Resolution Remote Sensing Models." *Photogrammetric Engineering & Remote Sensing* 73(8): 945–54.

Bell, D.M., J.T. Hunter, and R.J. Haworth. 2008. "Montane Lakes (Lagoons) of the New England Tablelands Bioregion." *Cunninghamia* 10(3): 475–92.

Campos, J.C., N. Sillero, and J.C. Brito. 2012. "Normalized Difference Water Indexes Have Dissimilar Performances in Detecting Seasonal and Permanent Water in the Sahara–Sahel Transition Zone." *Journal of Hydrology* 464–465: 438–46.

Carlson, T.N., and D.A. Ripley. 1997. "On the Relation between NDVI, Fractional Vegetation Cover, and Leaf Area Index." *Remote Sensing of Environment* 62(3): 241–52.

Chasmer, L., C. Mahoney, K. Millard, K. Nelson, D. Peters, M. Merchant, C. Hopkinson, et al. 2020. "Remote Sensing of Boreal Wetlands 2: Methods for Evaluating Boreal Wetland Ecosystem State and Drivers of Change." *Remote Sensing* 12(8): 1321.

Davidson, N.C. 2014. "How Much Wetland Has the World Lost? Long-Term and Recent Trends in Global Wetland Area." *Marine and Freshwater Research* 65(10): 934–41.

DeVries, B., C. Huang, M. Lang, J. Jones, W. Huang, I. Creed, and M. Carroll. 2017. "Automated Quantification of Surface Water Inundation in Wetlands Using Optical Satellite Imagery." *Remote Sensing* 9(8): 807.

Dudgeon, D., A.H. Arthington, M.O. Gessner, Z.-I. Kawabata, D.J. Knowler, C. Leveque, R.J. Naiman, A.-H. Prieur-Richard, D. Soto, and M.L. Stiassny. 2006. "Freshwater Biodiversity: Importance, Threats, Status and Conservation Challenges." *Biological Reviews* 81(2): 163–82.

Erwin, K.L. 2009. "Wetlands and Global Climate Change: The Role of Wetland Restoration in a Changing World." *Wetlands Ecology and Management* 17(1): 71.

Fisher, A., N. Flood, and T. Danaher. 2016. "Comparing Landsat Water Index Methods for Automated Water Classification in Eastern Australia." *Remote Sensing of Environment* 175: 167–82.

Foody, G.M. 2002. "Status of Land Cover Classification Accuracy Assessment." *Remote Sensing of Environment* 80(1): 185–201.

Gao, B.-C. 1996. "NDWI—A Normalized Difference Water Index for Remote Sensing of Vegetation Liquid Water from Space." *Remote Sensing of Environment* 58(3): 257–66.

Géron, A. 2017. *Hands-On Machine Learning with Scikit-Learn and TensorFlow: Concepts, Tools, and Techniques to Build Intelligent Systems*. Sebastopol, CA: O'Reilly Media, Inc.

Gorelick, N., M. Hancher, M. Dixon, S. Ilyushchenko, D. Thau, and R. Moore. 2017. "Google Earth Engine: Planetary-Scale Geospatial Analysis for Everyone." *Remote Sensing of Environment* 202: 18–27.

Hu, S., Z. Niu, Y. Chen, L. Li, and H. Zhang. 2017. "Global Wetlands: Potential Distribution, Wetland Loss, and Status." *Science of the Total Environment* 586: 319–27.

Hunter, J.T. 2021. "Vegetation Change in Semi-Permanent or Ephemeral Montane Marshes (Lagoons) of the New England Tablelands Bioregion." *Australian Journal of Botany* 69(7): 478–89.

Hunter, J.T., and A.M. Lechner. 2017. "A Multiscale, Hierarchical, Ecoregional and Floristic Classification of Arid and Semi-Arid Ephemeral Wetlands in New South Wales, Australia." *Marine and Freshwater Research* 69(3): 418–31.

Inman, V.L., and M.B. Lyons. 2020. "Automated Inundation Mapping over Large Areas Using Landsat Data and Google Earth Engine." *Remote Sensing* 12(8): 1348.

Jahncke, R., B. Leblon, P. Bush, and A. LaRocque. 2018. "Mapping Wetlands in Nova Scotia with Multi-Beam RADARSAT-2 Polarimetric SAR, Optical Satellite Imagery, and Lidar Data." *International Journal of Applied Earth Observation and Geoinformation* 68: 139–56.

Ji, L., L. Zhang, and B. Wylie. 2009. "Analysis of Dynamic Thresholds for the Normalized Difference Water Index." *Photogrammetric Engineering & Remote Sensing* 75(11): 1307–17.

Jones, J.W. 2015. "Efficient Wetland Surface Water Detection and Monitoring via Landsat: Comparison with In Situ Data from the Everglades Depth Estimation Network." *Remote Sensing* 7(9): 12503–38.

Kingsford, R.T., A. Basset, and L. Jackson. 2016. "Wetlands: Conservation's Poor Cousins." *Aquatic Conservation: Marine and Freshwater Ecosystems* 26(5): 892–916.

Kissel, A.M., M. Halabisky, R.D. Scherer, M.E. Ryan, and E.C. Hansen. 2020. "Expanding Wetland Hydroperiod Data Via Satellite Imagery for Ecological Applications." *Frontiers in Ecology and the Environment* 18(8): 432–8.

LaRocque, A., C. Phiri, B. Leblon, F. Pirotti, K. Connor, and A. Hanson. 2020. "Wetland Mapping with Landsat 8 OLI, Sentinel-1, ALOS-1 PALSAR, and LiDAR Data in Southern New Brunswick, Canada." *Remote Sensing* 12(13): 2095.

Lechner, A.M., N. McCaffrey, P. McKenna, W.N. Venables, and J.T. Hunter. 2016. "Ecoregionalization Classification of Wetlands Based on a Cluster Analysis of Environmental Data." *Applied Vegetation Science* 19(4): 724–35.

Lefebvre, G., A. Davranche, L. Willm, J. Campagna, L. Redmond, C. Merle, A. Guelmami, and B. Poulin. 2019. "Introducing WIW for Detecting the Presence of Water in Wetlands with Landsat and Sentinel Satellites." *Remote Sensing* 11(19): 2210.

Martinez, J.-M., and T. Le Toan. 2007. "Mapping of Flood Dynamics and Spatial Distribution of Vegetation in the Amazon Floodplain Using Multitemporal SAR Data." *Remote Sensing of Environment* 108(3): 209–23.

McFeeters, S.K. 1996. "The Use of the Normalized Difference Water Index (NDWI) in the Delineation of Open Water Features." *International Journal of Remote Sensing* 17(7): 1425–32.

Mohammadi, A., J.F. Costelloe, and D. Ryu. 2017. "Application of Time Series of Remotely Sensed Normalized Difference Water, Vegetation and Moisture Indices in Characterizing Flood Dynamics of Large-Scale Arid Zone Floodplains." *Remote Sensing of Environment* 190: 70–82.

Montgomery, J., B. Brisco, L. Chasmer, K. Devito, D. Cobbaert, and C. Hopkinson. 2019. "SAR and Lidar Temporal Data Fusion Approaches to Boreal Wetland Ecosystem Monitoring." *Remote Sensing* 11(2): 161.

Mueller, N., A. Lewis, D. Roberts, S. Ring, R. Melrose, J. Sixsmith, L. Lymburner, et al. 2016. "Water Observations from Space: Mapping Surface Water from 25 Years of Landsat Imagery across Australia." *Remote Sensing of Environment* 174: 341–52.

New South Wales Government. 2020. "Upland Wetlands of the Drainage Divide of the New England Tableland Bioregion – Profile." https://www.environment.nsw.gov.au/threatenedspeciesapp/profile.aspx?id=10824

NSW National Parks and Wildlife Service. 2003. *The Bioregions of New South Wales: Their Biodiversity, Conservation and History*. Hurstville, NSW, Australia: NSW National Parks and Wildlife Service.

Pedregosa, F., G. Varoquaux, A. Gramfort, V. Michel, B. Thirion, O. Grisel, M. Blondel, et al. 2011. "Scikit-Learn: Machine Learning in Python." *Journal of Machine Learning Research* 12: 2825–30.

Reid, A.J., A.K. Carlson, I.F. Creed, E.J. Eliason, P.A. Gell, P.T. Johnson, K.A. Kidd, T.J. MacCormack, J.D. Olden, S.J. Ormerod, and J.P. Smol. 2019. "Emerging Threats and Persistent Conservation Challenges for Freshwater Biodiversity." *Biological Reviews* 94(3): 849–73.

Reis, V., V. Hermoso, S.K. Hamilton, D. Ward, E. Fluet-Chouinard, B. Lehner, and S. Linke. 2017. "A Global Assessment of Inland Wetland Conservation Status." *Bioscience* 67(6): 523–33.

Roshier, D.A., and R.M. Rumbachs. 2004. "Broad-Scale Mapping of Temporary Wetlands in Arid Australia." *Journal of Arid Environments* 56(2): 249–63.

Rouse, J.W., H.H. Rüdiger, J.A. Schell, and D.W. Deering. 1974. "Monitoring Vegetation Systems in the Great Plains with ERTS." In NASA Special Publication 351, 309.

Saunders, M.E., D.S. Bower, S. Mika, and J.T. Hunter. 2021. "Condition Thresholds in Australia's Threatened Ecological Community Listings Hinder Conservation of Dynamic Ecosystems." *Pacific Conservation Biology* 27: 221–30.

Schael, D.M., P.T. Gama, and B.L. Melly. 2015. *Ephemeral Wetlands of the Nelson Mandela Bay Metropolitan Area: Classification, Biodiversity and Management Implications*, 233. Report to the Water Research Commission. WRC Report number 2181/1/15. Port Elizabeth, South Africa: Nelson Mandela Metropolitan University.

Storey, J., M. Choate, and K. Lee. 2014. "Landsat 8 Operational Land Imager on-Orbit Geometric Calibration and Performance." *Remote Sensing* 6(11): 11127–52.

Thomas, R.F., R.T. Kingsford, Y. Lu, S.J. Cox, N.C. Sims, and S.J. Hunter. 2015. "Mapping Inundation in the Heterogeneous Floodplain Wetlands of the Macquarie Marshes, Using Landsat Thematic Mapper." *Journal of Hydrology* 524: 194–213.

Thomas, R.F., R.T. Kingsford, Y. Lu, and S.J. Hunter. 2011. "Landsat Mapping of Annual Inundation (1979–2006) of the Macquarie Marshes in Semi-Arid Australia." *International Journal of Remote Sensing* 32(16): 4545–69.

Tulbure, M.G., and M. Broich. 2013. "Spatiotemporal Dynamic of Surface Water Bodies Using Landsat Time-Series Data from 1999 to 2011." *ISPRS Journal of Photogrammetry and Remote Sensing* 79: 44–52.

Wolski, P., M. Murray-Hudson, K. Thito, and L. Cassidy. 2017. "Keeping It Simple: Monitoring Flood Extent in Large Data-Poor Wetlands Using MODIS SWIR Data." *International Journal of Applied Earth Observation and Geoinformation* 57: 224–34.

Xu, H. 2006. "Modification of Normalised Difference Water Index (NDWI) to Enhance Open Water Features in Remotely Sensed Imagery." *International Journal of Remote Sensing* 27(14): 3025–33.

SUPPORTING INFORMATION

Additional supporting information may be found in the online version of the article at the publisher's website.

How to cite this article: Brinkhoff, James, Gillian Backhouse, Manu E. Saunders, Deborah S. Bower, and John T. Hunter. 2022. "Remote Sensing to Characterize Inundation and Vegetation Dynamics of Upland Lagoons." *Ecosphere* 13(1): e3906. https://doi.org/10.1002/ecs2.3906